Paper presented at Dynamics and Control of Systems and Structures in Space (DCSSS),
5th conference, Kings College, Cambridge, July 2002

Performance Comparison of Reusable Launch Vehicles

Mark Ayre, Tom Bowling, Cranfield University, Bedfordshire, MK43 OAL.

Abstract

A parameterised generic launch vehicle design is subjected to performance evaluation using the ORBITER model which is capable of optimising both the design and trajectory of the vehicle. The launcher initial mass, flight path angle, velocity and altitude are varied around design points of existing vehicle concepts to investigate the subsequent effect on performance for payload delivery into a 90km by 200km orbit. The performance results suggest that SSTO systems are unfeasible, delivering marginal positive payload performance only when externally accelerated to high speed using a sled mechanism. The optimal vehicle type from a purely performance perspective is deemed to be the TSTO vertically launched configuration.

Introduction

The requirement for cheap access to space is now widely accepted [1]. Reusable launch vehicles are seen as the key to cost reduction through various benefits including increased reliability, incremental testing and maintenance, operations and materials savings. Much work has been conducted worldwide in reusable launch vehicle performance comparison [2,3,4]. Performance comparison requires that design and trajectory of a launch vehicle be optimised in tandem, due to the strongly coupled relationship between vehicle design and trajectory. The ORBITER model provides such a capability.

Vehicle Geometry

The vehicle design is defined by a number of user-supplied design constants, and eleven design parameters which, along with the trajectory parameters, form the optimisable parameter vector (in **Optimisation** section). The basic vehicle geometry and the eleven optimisable design parameters are defined in Figure 1.

The fuselage (f, e, h_b, l_h) is modelled by a power law fairing curve, with a blunted nose, and an elliptical cross-section. It is broken down into five main sections: the nose, the equipment bay, the main hydrogen tank, intertank area, and the engine bay. The fuselage is sized by considering each of these sections separately. The wing (c_r, c_t, t/c, b) is defined by four design parameters (see Figure 1), and the wing position relative to the fuselage is given by x_{root}. The engine sizing is controlled by the design parameter e_{scale}, and the TPS weight is determined from the design heat load, q_{design}.

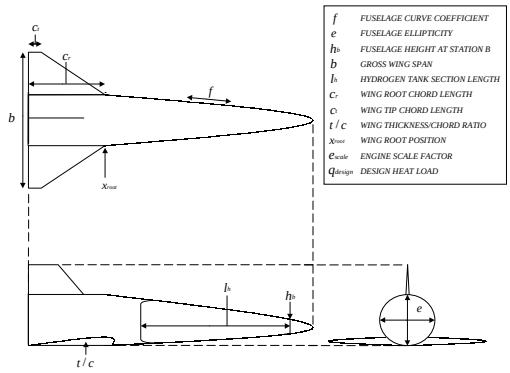

Figure 1: The parametric definition of the generic launch vehicle design

Flight Dynamics

A 3 degree of freedom model over a rotating Earth is used to model the vehicle's ascent and descent. The launcher is considered to be a point mass for the purposes of the trajectory simulation (all forces are assumed to act through the centre of mass of the vehicle, with no provision made for turning moments). Vehicle position is defined by a geocentric spherical co-ordinate system which rotates with the Earth. The atmosphere is assumed to rotate with the Earth, so windshear effects are not considered. Vehicle position is described by the following three state variables:

- Geocentric radius of the vehicle, $\underline{r}$, measured from the centre of the Earth to the launcher.
- Latitude of the vehicle, Φ, defined as the angle at the centre of the Earth between the position vector to the vehicle and the plane of the equator.
- Longtitude of the vehicle, λ, defined as the angle between the Greenwich Meridian and the great circle passing over both poles and through the point mass of the vehicle.

The velocity vector is defined relative to a horizontal plane local to the launcher. Three state variables describe the velocity vector:

- The speed relative to the Earth, $\underline{V}$.
- The flight path angle, γ, defined as the angle between the velocity vector and the local horizontal.

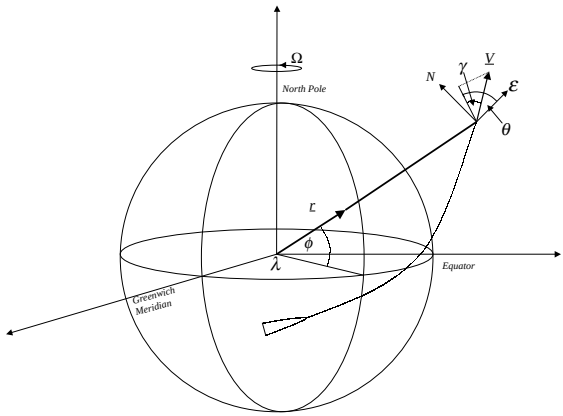

Figure 2: The celestial geometry of the orbiter trajectory

- The heading angle, θ, defined as the angle between the local parallel of latitude and the component of the velocity vector which lies in the local horizontal plane.

In addition to these six states, the mass of the vehicle, m, is added. The aerodynamic forces on the vehicle are described by

$$L = qSC_L \tag{1}$$

$$D = qSC_D \tag{2}$$

where q is the dynamic pressure and S is the aerodynamic reference area. Lift and drag coefficients are obtained from the aerodynamic routines (see section **Aerodynamics**) as functions of incidence, mach number and vehicle geometry. Along with the dynamic pressure and aerodynamic reference area, this then allows the sizes of the aerodynamic forces to be determined.

Maximum thrust is determined as a function of altitude, atmospheric pressure, engine vacuum thrust and nozzle exit area. The throttle parameter u allows the magnitude of the thrust vector to be altered, and is in the range [0,1]. Trajectory control is effected by the incidence and roll angles, and the throttle setting. These determine the direction and magnitude of the thrust and aerodynamic forces. The incidence is the angle between the vehicle centreline and the velocity vector. The roll angle is measured from the axis parallel to the vertical fin in a clockwise direction. Incidence

alters the size of both the lift and drag forces, whilst the roll angle effects only the direction of the lift vector with respect to the local vertical.

Control is assumed to act instantaneously. At any given time, t, the control angle (angle of attack) is found by linear interpolation between the two control angle values at the time nodes immediately before and after t. The thrust vector is set at a constant angle to the vehicle centreline, specified by the user (no allowance is made for thrust gimballing). Heating is modelled by the total kinetic heating encountered by a unit sphere located at the nose stagnation point: this is used to measure the re-entry heating independent of the geometry of the vehicle.

Engine Modelling

The engine model treats the thrust as a factor (given by e_{scale}) of the baseline engine defined by the user. User-supplied design constants are T_0, the vacuum thrust, $\dot{m}_0$, the maximum massflow rate, S_0, the baseline nozzle exit area and σ_{engine}, the engine scale factor (optimisable parameter). The maximum thrust at any altitude is given by

$$T_{\max} = \sigma_{engine}\,(T_0 - S_0 p) \tag{3}$$

where p is the atmospheric pressure. T_{max} is then multiplied by u, the throttle parameter to give the actual thrust (the engine is assumed to be at full thrust unless the longtitudinal acceleration constraint is violated (see section **Optimisation**)).

Mass Estimation

The take-off mass of the vehicle is broken down into three components

$$m_{to} = m_{dry} + m_{fuel} + m_{pay} \tag{4}$$

Where m_{to} is the take-off mass, m_{dry} is the dry mass of the vehicle (i.e. unfueled), m_{fuel} is the mass of the fuel carried and m_{pay} is the payload mass. The Gross Lift-Off Mass (GLOM) is taken to be the mass of the vehicle at the start of the ascent trajectory (i.e. immediately after stage separation or lift-off from the ground, i.e. in the case of two stage vehicles only the upper stage is modelled). The dry mass, m_{dry}, is fixed by the values of the design parameters and design constants supplied by the user. The fuel mass (assumed LOX/LH2 combination) is also evaluated from the design parameters. Thus only the payload mass, m_{pay}, and GLOM, m_{to}, are unknown from equation (4). Mass Estimation Relationships (MERs) derived from past RLV design projects are used to estimate the mass of the launch vehicle.

The propellant mass is divided into four components; the mass of fuel available for ascent, the mass of wasted fuel (ullage, residuals etc.), and the mass of propellant required for the OMS and RCS systems

$$m_{fuel} = m_{fav} + m_{waste} + m_{OMSprop} + m_{RCSprop} \tag{5}$$

The mass of LH2 is calculated from considering the size of the fuselage section containing the fuel tank, then determining the size of the fuel tank itself, using volume efficiency factors to model the maximum packing efficiency and effects of cross-sectional ellipticity. The mass of LOX is assumed to be that required to burn all the LH2. Both the OMS and RCS fuel budgets are determined from the ideal rocket equation ($\Delta V = I_{sp} g ln R$), using user supplied values of the ΔV requirement and the specific impulse of each system. No allowance for propellant loss is made in the OMS/RCS systems.

Aerodynamics

The calculation of the vehicle aerodynamics is divided into routines which calculate the launcher lift and drag coefficients (C_L and C_D) in the sub/supersonic, transonic and hypersonic regimes, to be used in equations (1) and (2).

The subsonic aerodynamics estimation routines use a mixture of theoretical and empirical methods, and are applied up to mach 2.85. Between mach 2.85 and mach 5.0 (the beginning of the hypersonic regime) the aerodynamic coefficient values are interpolated between calculated supersonic and hypersonic values. The lift of the launcher is found using an estimation of the lift curve slope (LCS) for the vehicle in three flight regimes. The lift coefficient, C_L, is then given by:

$$C_L = \alpha \frac{\partial C_L}{\partial \alpha} \tag{6}$$

This assumes that LCS is constant with respect to angle of attack. According to the current mach number, the estimation of the vehicle LCS is divided into subsonic, transonic and supersonic cases. In each case, the contribution from the body and the wing are considered separately and then combined to produce the Lift Curve Slope.

The drag component of the sub/supersonic regimes is estimated by evaluating the three components of the drag (Zero-lift drag, Wave drag, Lift-dependent drag) separately. In the hypersonic regime, the aerodynamics of the launcher are calculated using known analytical solutions for a number of simple geometric shapes using a Newtonian flow approximation.

In order to calculate the dynamic pressure, and hence find the aerodynamic forces from (1) and (2), as well as the engine thrust from (3), several atmospheric parameters must be calculated (density, pressure and speed of sound). Therefore a standard tropical atmosphere model is used, assuming the air obeys the perfect gas law and the equation of hydrostatic equilibrium.

Optimisation

Generally, for the launcher optimal control problem, we desire the solution which maximises an objective function, $J(\underline{u})$, subject to two sets of constraints

$$\begin{aligned} C_1(\underline{u}) &= 0 \\ C_2(\underline{u}) &\leq 0 \end{aligned} \tag{7}$$

The constraints are divided into equality (C_1) and inequality (C_2) constraints (for example, longtitudinal and normal acceleration limits, integrated heat loads, peak heating values etc.). The optimiser is provided with the first order gradients of the objective function and constraints with respect to the elements of the parameter vector. For an explicit description of the optimisation algorithm, refer to [5]. The form of the objective function is such that variation of the optimisation condition is possible. The objective function has the form:

$$J = \frac{\alpha_1 m_{payload} + \alpha_2 m_{vehicle} + \alpha_3 m_{fuel}}{\alpha_4 m_{payload} + \alpha_5 m_{vehicle} + \alpha_6 m_{fuel} + \alpha_7} + \alpha_8 m_{ascent} + \alpha_9 q_{actual} \tag{8}$$

The α terms are user-defined coefficients that can supress part of the objective function (i.e. by setting the α terms to 1 or 0). Manipulation of the objective function in this way thus allows the user to select several different mass fractions as the objective function by which to perform the optimisation (α_7 is included to avoid the denominator being set to zero).

Comparison

Seven vehicle concepts were studied through selection of initial conditions which were representative of that concept. The seven concepts are denoted:

SSTOHLHL - Single Stage Horizontal Launch and Landing.

SSTOSLHL - Single Stage Horizontal Launch and Landing (sled).

SSTOVLVL - Single Stage Vertical Launch and Landing.

SSTOVLHL - Single Stage Vertical Launch and Horizontal Landing.

TSTOVLHL - Two Stage Vertical Launch and Horizontal Landing.

TSTOHLHL(sub) - Two Stage Horizontal Launch and Landing (subsonic sep.).

TSTOHLHL(sup) - Two Stage Horizontal Launch and Landing (supersonic sep.).

For the two stage vehicle concepts, the first stages were assumed, taken from quoted performance and mass characteristics of the SL-86, Sanger, Interim HOTOL and a reusable booster [6,7,8,9]. Initially, a baseline vehicle design was produced, with

Configuration	GLOM masses/ tonnes	initial velocity/ ms^{-1}	flight path angle/ $^\circ$	altitude/ km
SSTOHLHL	250, 400, 600	100	0	0.01
SSTOSLHL	250, 400, 600	100 and 250	0 to 10	0.01
SSTOVLVL	250	0	90	0.01
SSTOVLHL	250, 400, 600	0	90	0.01
TSTOVLHL	250, 188	1920.6	21	30
TSTOHLHL(sub)	250	250	0	9.2
TSTOHLHL(sup)1	250, 115	1188.2	0	24
TSTOHLHL(sup)2	250, 96	1920.6	0	30

Table 1: Summary of initial conditions used in the comparative study

the GLOM fixed at 250 tonnes. GLOM was also varied to the design masses of upper stages from the TSTO concepts, and increased to 400 and 600 tonnes for the SSTO vehicles. Performance comparison was conducted over a range of initial mass, flight path angle, altitude and speed conditions, with a number of constraints applied (longtitudinal and normal acceleration limits, leading edge temperature limits etc.) including a reentry cross-range of 10° and a landing field length limit of $3500m$. The seven configurations, and the intitial conditions given to them are shown in table 1.

Results

Table 2 summarises the main results, giving the vehicle performance along with a gross summary of the vehicle design in terms of mass fractions. Figure 3 shows an example output for the TSTOVLHL configuration.

Discussion and Conclusions

Referring to table 2, SSTO vehicles are shown to have generally poor performance. SSTOHLHL vehicles all deliver highly negative payloads, primarily due to the mass penalty associated with an undercarriage which has to support the GLOM of the vehicle, coupled with a large wing mass fraction due to the size of wing required to allow rotation at $100ms^{-1}$, approximately the upper limit of speeds which can be achieved with conventional tyred undercarriage. The sled-launched SSTOSLHL (which is externally accelerated) delivers reasonable payloads at a rotation speed of $250ms^{-1}$, however, this corresponds to a sea-level mach number in excess of 0.7 and is not thought to be practically achievable. At the lower rotation speed of $100ms^{-1}$ marginally positive payloads are achieved at higher GLOM values.

The ballistic (SSTOVLVL) vehicle analysis suggests that the mass of fuel required for controlled landing using reigniteable main engines would probably be at least as much as wings. Additional complexity in the pressurisation and feed systems of

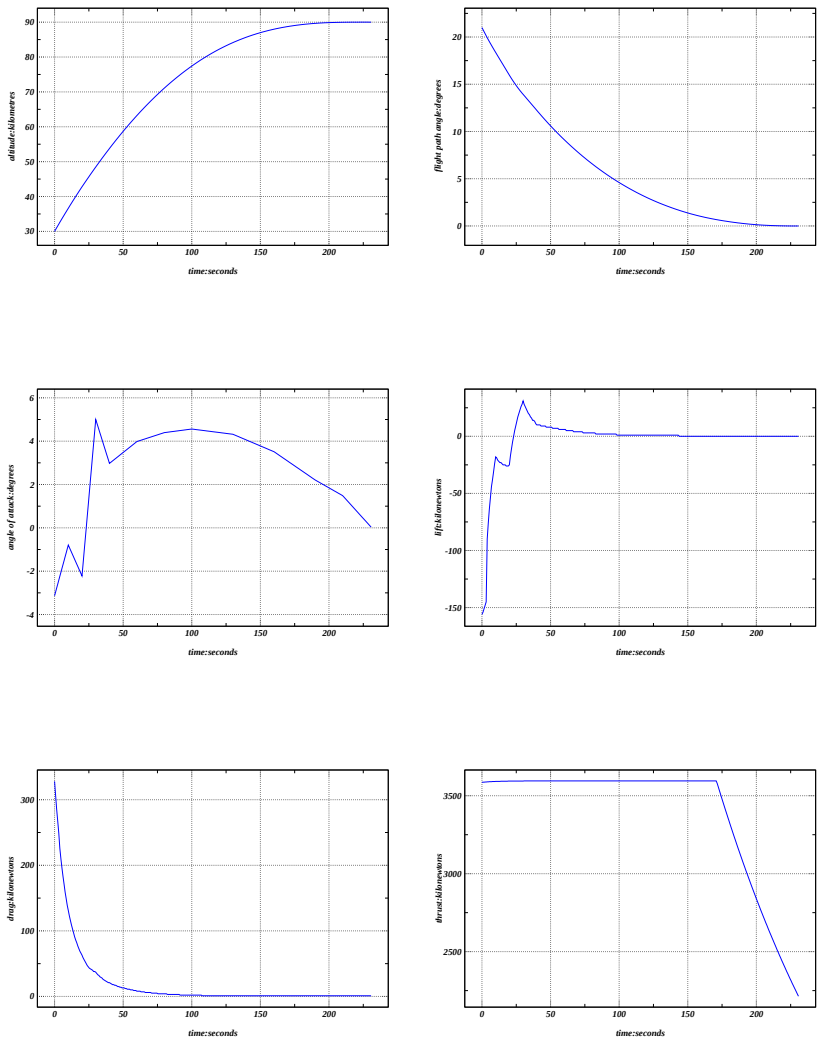

Figure 3: Altitude, flight path angle, angle of attack, lift, drag and thrust against time for the TSTOVLHL optimised vehicle

GLOM/tonnes	Payload Mass/kg	Payload Mass Fraction	Fuel Mass Fraction	Structural Coefficient	Payload/ Vehicle Fraction	Wing mass fraction	Engine mass fraction
SSHLHL							
250	-14873.5	-5.95	86.81	19.14	-	11.54	12.77
400	-20426.5	-5.11	86.79	18.40	-	11.17	14.08
600	-29699.4	-4.95	86.59	18.36	-	11.91	14.71
SSHLHL(sled)							
250(250ms^{-1})	175.9	0.07	86.54	13.39	0.52	11.51	18.26
400(250ms^{-1})	3585.6	0.90	86.62	12.48	6.70	13.12	20.67
600(250ms^{-1})	8054.9	1.34	86.75	11.91	10.13	14.33	22.68
250(100ms^{-1})	-3454.3	-1.38	87.35	14.03	-	13.83	17.42
400(100ms^{-1})	115.5	0.03	87.28	12.69	0.23	14.20	20.32
600(100ms^{-1})	2670.1	0.45	87.40	12.15	3.66	15.53	22.22
SSVLHL							
250	-4858.8	-1.94	88.09	13.86	-	10.35	21.10
400	-4008.7	-1.002	88.04	12.96	-	11.84	23.79
600	-2837.4	-0.47	88.06	12.42	-	12.94	26.01
SSVLVL							
250	-4443.6	-1.78	87.98	12.36	-	0.0	23.66
TSVLHL							
250	27547.9	11.02	74.23	14.75	42.76	15.68	19.00
188	19516.4	10.38	74.40	15.22	40.54	15.66	15.82
TSHLHL(sub)							
250	4074.2	1.63	85.48	12.89	11.22	12.76	15.58
TSHLHL(sup)							
250	13111.7	5.25	81.04	13.72	27.66	14.40	17.98
115	1931.3	1.68	81.10	17.22	8.89	12.00	14.90
96	4493.0	4.68	76.94	18.38	20.30	12.41	12.66

Table 2: Summary of optimised baseline vehicle performance and mass characteristics for each configuration (for TSTO vehicles, the values shown are for the second stage only)

the engine to ensure the degree of restart and throttle control required would push the mass penalty up further. The SSTOVLHL configuration is unable to deliver a positive payload to orbit for all the GLOM values studied, although the negative payload fraction does approach zero as the GLOM is increased, again evidence of the importance of scaling effects.

Generally, TSTO configurations have a much better performance; The fundamental advantage of not having to accelerate the entire structural mass of the vehicle to orbital velocity is unavoidable and asserts itself here. Of the TSTO configurations, the one which delivers the best payload performance is (TSTOVLHL); the benefit of staging at the optimum flight path angle are shown to be considerable, adding approximately 20% to the payload delivered when compared to equivalent velocity and altitude separation conditions at zero flight path angle. This fractional increase in payload decreases as separation altitude increases due to the reduction in the difference between the horizontal and optimum flight path angles.

The supersonic separation (TSTOHLHL (sup)) (of which two design points have been studied) does not give any significant performance improvement over (TSTOHLHL (sub)). The benefits of staging at a higher mach number and altitude are largely cancelled out by the higher structural mass fraction associated with a smaller second stage. There exist considerable structural penalties (a result of loss of volumetric efficiencies) when vehicle GLOM is scaled downwards. Because of this (TSTOHLHL (sub)), which separates at 250 tonnes, is able to compare favourably, in terms of payload to orbit, with (TSTOHLHL (sup)) despite the much lower altitude and speed at which it separates. This scaling effect will have to be very carefully considered in future detailed design work. First stage size and performance has to date largely been constrained by runway length; The faster and higher the separation point, the smaller the upper stage mass.

Summary

The TSTOVLHL configuration is shown to give the best performance; this is due to the considerable performance improvement (over TSTOHLHL configurations) engendered by separation at the optimum flight path angle. SSTO configurations are shown to have marginal or negative payload performance, and display a high sensitivity to scaling. Scaling effects are shown to be important generally, and not something that can be ignored in comparative analysis.

References

[1] Koelle, D. E., Launch Cost as Design Tool - Cost as Principal Vehicle Concept Design and Selection Criteria. *Proceedings from the 44th IAF Congress*. IAA 1.1-93-645, 1993

[2] Shkadov, L., M., Denisov, V. Ye., Lazarev, V. V., Plokhikh, V. P., Buzuluk, V. I., Volodin, S. V., Cervonenko, K. A., Skipenko, V. V., The Comparative Analysis of Various Aerospace System Concepts. *Acta Astronautica*, vol. 35, no. 1, pp.47-54, 1995

[3] Stanley, D. O., Wilhite, A. W., Englund, W. C., Comparison of Single-Stage and Two-Stage Airbreathing Launch Vehicles. *Journal of Spacecraft and Rockets*, vol. 29, no. 5, pp.735-740, 1992

[4] Freeman, D. C., Talay, T. A., Stanley, D. O., Lepsch, R.A., Wilhite, A. W., Design Options for Advanced Manned Launch Systems. *Journal of Spacecraft and Rockets*, vol. 32, no. 2, pp.241-249, 1994

[5] McGregor, A. E., A Combined Design and Trajectory Optimisation Algorithm for an Orbiter Vehicle, Cranfield University, UK, 1995

[6] Fielding, J., The SL-86 Launch System, *Cranfield College of Aeronautics Internal Report*, 1986

[7] Koelle, D., Advanced Two Stage Vehicle Concepts (SANGER). *AIAA/ SAE/ ASME/ ASEE 26th Joint Propulsion Conference*, AIAA-90-1933, 1990

[8] Parkinson, R., The An-225/Interim HOTOL Launch Vehicle. *Proceedings from the 3rd International Aerospaceplanes Conference*, AIAA-91-5006, 1991

[9] Terrenoire, P., Masse, B., Prager, G., An Overview of the Reusable Rocket Launchers based on Near Term Technologies. *Proceedings from the 46th International Astronautical Federation Congress*, IAF-94-V.3.539, 1994